

STANISŁAW WOLNY*

**DYNAMIC LOADING OF MINING HOIST ELEMENTS IN THE VIEW OF THE EXPERIMENT
PERFORMED DURING REGULAR OPERATION OF THE REAL OBJECT**

**OBCIĄŻENIA DYNAMICZNE ELEMENTÓW GÓRNICZEGO URZĄDZENIA WYCiąGOWEGO
W CZASIE JEGO NORMALNEJ EKSPLOATACJI W ŚWIETLE EKSPERYMENTU NA OBIEKCIE
RZECZYWISTYM**

In the paper is presented the analysis focused on determination of forces in suspensions of tubs and counterbalance ropes in regular operation conditions. The particular attention has been taken to the phase of the hoist start with the input displacement applied to the drive wheel. Displacements and stresses in any section of lifting and counterbalance ropes are determined for such a situation. Moreover these results have been verified in the experiment in the real hoist installation. This experiment has been limited to the measurement of forces in the suspension of the tub, which starts from the shaft bottom with constant acceleration. Determined values of loads of the tub elements in operational condition could be useful as the basis for the strength analysis of elements.

Key words: mining hoist, dynamics, loads

Urządzenia wyciągowe w kopalniach są budowane i stosowane od wielu lat. Są one tematem ciągłych badań, których celem jest poznanie czynników umożliwiających poprawę ich własności eksploatacyjnych. Mimo to, obowiązujące obecnie kryteria wymiarowania i projektowania elementów naczynia wydobywczego nie odzwierciedlają pełnej specyfiki warunków pracy górniczego urządzenia wyciągowego. Stosowana metoda naprzężen dopuszczalnych umożliwia jedynie ocenę ich nośności, nie daje natomiast możliwości określenia ich trwałości zmęczeniowej.

Przepracowanie nowych kryteriów obliczeń wybranych elementów naczynia wydobywczego wymagać będzie zatem:

1. Przeprowadzenia kompleksowej analizy dynamicznej pracy urządzenia wyciągowego w czasie normalnej eksploatacji, jak również w stanach awaryjnych, zweryfikowanych pomiarami obciążień wybranych elementów tego układu na obiekcie rzeczywistym.

2. Wykonania szczegółowej analizy wytrzymałościowo-zmęczeniowej wybranych elementów urządzenia wyciągowego z wykorzystaniem rzeczywistych przebiegów zmienności ich obciążenia.

* ZAKŁAD WYTRZYMAŁOŚCI MATERIAŁÓW I KONSTRUKCJI, AKADEMIA GÓRNICZO-HUTNICZA, 30-059 KRAKÓW,
AL. MICKIEWICZA 30

Rozważania zawarte w tym opracowaniu koncentrują się na części punktu 1, a dotyczą wyników analizy pracy górnego urządzenia wyciągowego w czasie jego normalnej eksploatacji. Wyniki tej analizy wraz z rozważaniami zawartymi w innych pracach (Wolny 2000a, b, 2001; Wolny, Kjuregjan 1999) w całości wyczerpują treści zawarte w punkcie 1. Szczegółowym badaniom, podobnie jak w pracy Wolnego (2001), poddano obciążenia zawieszeń naczyni wydobywczych, na tle wyników eksperymentu przeprowadzonego na obiekcie rzeczywistym w przypadku rozruchu naczynia pełnego, podnoszonego z dolnego poziomu załadowczego ze stałym przyspieszeniem rozruchu. Dla tej fazy pracy urządzenia wyciągowego, układ zastąpiono modelem jak na rysunku 3. Dla przyjętego modelu zapisano równania ruchu elementów lin (nośnych i wyrównawczych) jak dla ciegną sprężystego (1). Następnie, korzystając z metod analitycznych, rozwiązyano równania z uwzględnieniem odpowiednich warunków początkowych i brzegowych. Otrzymane w postaci jawniej wzory określają przemieszczenia wybranych przekrojów lin (8) (9), jak również ich obciążenia (13) dla analizowanej fazy pracy urządzenia wyciągowego. Bazując na zależności (13) analizowano:

- a) wpływ przyspieszenia rozruchu na wartość nadwyżki dynamicznej w zawieszeniu naczynia,
- b) wpływ masy całkowitej na wartość nadwyżki dynamicznej w zawieszeniu naczynia podczas jego podnoszenia z podszybia,
- c) wpływ długości liny nośnej na wartość nadwyżki dynamicznej obciążenia zawieszenia naczynia w przypadku jego podnoszenia ze stałym przyspieszeniem.

Uzyskane na drodze teoretycznej rezultaty charakteryzujące proces podnoszenia naczynia z dolnego poziomu ze stałym przyspieszeniem rozruchu zostały zweryfikowane drogą pomiarów wybranych wielkości na obiekcie rzeczywistym. Eksperyment — z uwagi na trudności natury technicznej — ograniczono do pomiaru sił w zawieszeniu naczynia załadowanego w pełnym cyklu eksploatacyjnym.

Uzyskane rezultaty charakteryzujące proces rozruchu naczynia z podszybia ze stałym przyspieszeniem będące wynikiem analizy teoretycznej, zweryfikowane eksperymentem na obiekcie rzeczywistym, potwierdziły zasadność wprowadzonych założeń upraszczających. Wyniki pomiarów sił w zawieszeniu naczynia podczas jego rozruchu (rys. 16 i 17) skonfrontowane z wynikami analizy teoretycznej wykazują zadowalającą z technicznego punktu widzenia zgodność (różnice ekstremalne w granicach 4÷5%). Nadwyżka dynamiczna obciążenia w zawieszeniu naczynia podczas jego podnoszenia ze stałym przyspieszeniem waha się w granicach kilkunastu procent (rys. 14 i 15), w skrajnych przypadkach od 10 do 20%. Oznacza to, że obciążenie zawieszenia naczynia podczas jego rozruchu, szczególnie dla głębszych szybów, w sposób istotny nie wpłynie na kształt obciążenia naczynia w normalnym cyklu eksploatacyjnym (rys. 11).

Generalnie zatem należy stwierdzić, że zarówno hamowanie manewrowe, jak i rozruch naczynia z podszybia wprowadza do cyklu normalnej eksploatacji „zaburzenie” nie powodując jednak jego istotnej zmiany z punktu widzenia obliczeń wytrzymałościowo-zmęczeniowych.

Słowa kluczowe: górnicze wyciągi szybowe, dynamika, obciążenie

1. Introduction

The estimation of durability (the period of safe operation) of some specific elements of mining hoist has to be preceded by the strength-fatigue analysis regarding the variability of operational loading. Diagrams of loading will be determined after dynamical analysis of the mining hoist operation in the regular work conditions.

Dynamic analysis of the mining hoist installation in various phases of operation is also presented in other reports: Knop (1975), Wolny, Kjuregjan (1999), Wolny (2000a, b, 2001). In Knop (1975) and Wolny (2000a, 2001) is analysed dynamic loading of some elements of the hoist installation in the state of operational braking, when

emergency braking problems are presented in reports Wolny, Kjuregjan (1999) and Wolny (2000b).

Fig. 1 shows the model of the mining hoist that has been used for dynamic analysis described in those reports.

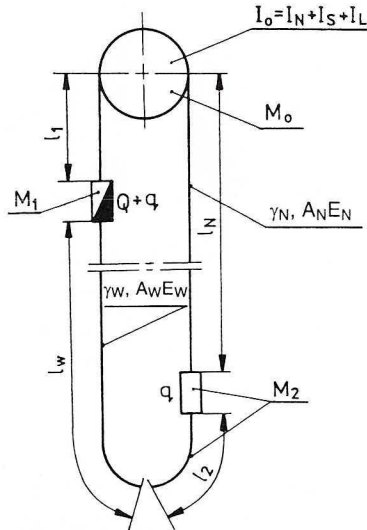


Fig. 1. Model of the hoist facility

M_1 — mass of the tub with the output, M_0 — reduced masses rotating in the tower, M_2 — reduced masses of the hoist in the sump, l_1 — length of supporting ropes between the upper tub and the drive wheel, l_w — length of balance ropes, l_N — length of supporting ropes, $A_w E_w, A_N E_N$ — tension rigidity of balance ropes and supporting ropes, γ_w, γ_N — linear desity of balance ropes and supporting ropes

Rys. 1. Model urządzenia wyciągowego

In this paper is presented the study of loads of some mining hoist elements in the regular operation cycle. Three phases in the cycle were distinguished, which are as follow:

- starting of the full tub from the shaft bottom,
- steady-state run of the full tub,
- braking of the tub, which reaches the shaft top.

Problems considered in Knop (1975), Wolny, Kjuregjan (1999) and Wolny (2000a, b, 2001) could be significantly simplified when the velocity function of the rope end, which is the mass M_0 (Fig. 1) in the considered case — has been assumed.

Then, the assembly shown in fig.1 may be separated into two independent sets as shown in Fig. 2. Due to experience (Knop 1975), there are reasons to legitimate this simplification. As a rule, the modern hoist installations are equipped with high power drive machines of the hard performance characteristics what makes possible to maintain the velocity, which follows presumed running-time diagram. Diagrams presented in Fig. 11 confirm it.

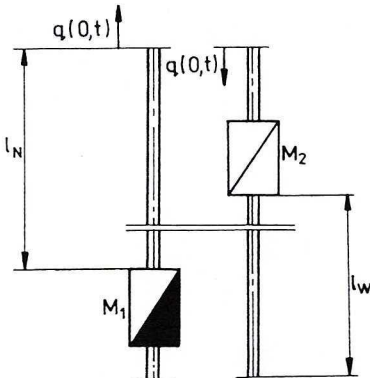


Fig. 2. Separation of the hoist facility into two independent systems in the case of the set value of driving wheel velocity

Rys. 2. Rozdział modelu urządzenia wyciągowego na dwa niezależne układy w przypadku zadanej prędkości koła pędnego

2. Forces in suspensions of tubs and counterbalance ropes caused by kinematic inputs (starting of the loaded tub from the shaft bottom)

Let us consider the model of the system, as shown in Fig. 3. It is the case when the mass M_2 is being elevated from the bottom extreme position. Let denote the function describing displacement of the rope end (circumferential displacement of the driving wheel) as $q(t)$.

Now, when the displacement of the balance rope cross-section in the abscissa y_1 is denoted as $v_1(y_1, t)$ we have the motion equation:

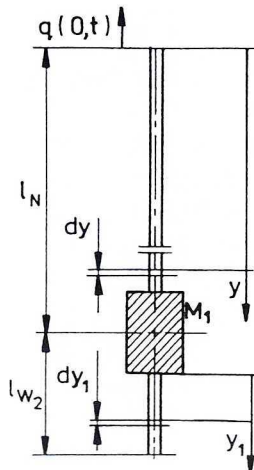


Fig. 3. Model of the hoist with the presumed velocity function of the upper end of the rope

Rys. 3. Model wyciągu z zadaną funkcją prędkości górnego końca liny

$$\frac{\partial^2 v(y, t)}{\partial t^2} - a_N^2 \frac{\partial^2 v(y, t)}{\partial y^2} = 0 \quad (1)$$

$$\frac{\partial^2 v_1(y_1, t)}{\partial t^2} - a_W^2 \frac{\partial^2 v_1(y_1, t)}{\partial y_1^2} = 0$$

which follows boundary conditions

$$v(y=0, t) = q_{(t)} \quad (2a)$$

$$M_2 \frac{\partial^2 v(y=l_N, t)}{\partial t^2} = A_W E_W \frac{\partial v_1(y_1=0, t)}{\partial y_1} - A_N E_N \frac{\partial v(y=l_N, t)}{\partial y} \quad (2b)$$

$$v_1(y_1=0, t) = v(y=l_N, t) \quad (2c)$$

$$\frac{\partial v_1(y_1=l_{W_r}, t)}{\partial y_1} = 0 \quad (2d)$$

where:

$q_{(t)}$ — the known time function.

Then we can look for the solution of equation (1) having the form (Kaliski 1987):

$$v(y, t) = f_0\left(t - \frac{y}{a_N}\right) + g_0\left(t + \frac{y}{a_N}\right) \quad (3a)$$

$$v_1(y_1, t) = \varphi_0\left(t - \frac{y_1}{a_W}\right) + \psi_0\left(t + \frac{y_1}{a_W}\right) \quad (3b)$$

The calculation procedure is significantly complicated, owing to the specific feature of d'Alembert method and the necessity of resolving the system of equation (1) in the subsequent time intervals relevant to periods required for the transition of the elastic deformation wave between boundaries of the continuum. In the model of the system there are lifting and counterbalance ropes and it is necessary to determine functions relevant to each rope and in all intervals of their lengths. Practically, it is not possible to obtain the general solution in such a way as there is an unlimited number of combinations of the counterbalance and lifting ropes lengths, what does affect the solution procedure itself. Therefore, the infinite length of the counterbalance rope has been assumed initially, and the number of functional forms was limited only to intervals resulting from the lengths of lifting ropes (3a). Regarding on (3a) and (3b) in relations (1) the formulae describing the function $f_0, g_0, \varphi_0, \psi_0$ were obtained in different intervals

of the plane of variables and namely: (t,y) for the supporting rope and (t,y_1) for the balance.

After substitution:

$$\frac{A_N E_N}{M a_N} = h, \quad \frac{A_W E_W}{M a_W} = h_1 \quad (4)$$

and regarding that:

$$h_r = h - h_1, \quad h_s = h + h_1, \quad l_N = l \quad (5)$$

these functions will obtain the general form (limited to the lifting rope in this report):

$$g_0\left(t + \frac{y}{a_N}\right) = \frac{a}{h_s^2} \left[h_s \left(t + \frac{y-2l}{a_N} \right) \left(1 + \frac{h_r}{h_s} \right) - \frac{1}{2} \left(t + \frac{y-2l}{a_N} \right)^2 (h_r, h_s) - \left(1 - e^{-h_s \left(t + \frac{y-2l}{a_N} \right)} \right) \right]. \quad (6)$$

$$\cdot u \left(t + \frac{y-2l}{a_N} \right) + \frac{a}{h_s^2} \left[-\frac{2(h_r h_s + h_r^2)}{h_s} \left(t + \frac{y-4l}{a_N} \right) + \frac{h_r^2}{2} \left(t + \frac{y-4l}{a_N} \right)^2 + \right. \\ \left. + \frac{4h_r h_s + 3h_r^2 + h_s^2}{h_s^2} \left(1 - e^{-h_s \left(t + \frac{y-4l}{a_N} \right)} \right) - \left(\frac{h_r}{h_s} + 1 \right)^2 h_s \left(t + \frac{y-4l}{a_N} \right) e^{-h_s \left(t + \frac{y-4l}{a_N} \right)} \right].$$

$$\cdot u \left(t + \frac{y-4l}{a_N} \right) - \frac{a}{h_s^2} \left[\frac{3h_r^2 + 3h_r^3}{h_s^2} \left(t + \frac{y-6l}{a_N} \right) - \frac{h_r^3}{h_s} \frac{1}{2} \left(t + \frac{y-6l}{a_N} \right)^2 - \right. \\ \left. - 3 \frac{3h_r^2 h_s + 2h_r^3 + h_r h_s^2}{h_s^3} \left(1 - e^{-h_s \left(t + \frac{y-6l}{a_N} \right)} \right) + 3h_r \left(\frac{h_r}{h_s} + 1 \right)^2 \left(t + \frac{y-6l}{a_N} \right) e^{h_s \left(t + \frac{y-6l}{a_N} \right)} + \right. \\ \left. + \frac{1}{2} h_s^2 \left(\frac{h_r}{h_s} \right)^3 \left(t + \frac{y-6l}{a_N} \right)^2 e^{-h_s \left(t + \frac{y-6l}{a_N} \right)} \right] u \left(t + \frac{y-6l}{a_N} \right)$$

$$\begin{aligned}
f_0 \left(t - \frac{y}{a_N} \right) = & -\frac{a}{2} \left(t - \frac{y}{a_N} \right)^2 - \frac{a}{h_s^2} \left[h_s \left(t - \frac{y+2l}{a_N} \right) \left(1 + \frac{h_r}{h_s} \right) - \frac{1}{2} \left(t - \frac{y+2l}{a_N} \right)^2 \right] \\
& \cdot (h_r h_s) + \left[-1 + e^{h_s \left(t - \frac{y+2l}{a_N} \right)} \right] \left(1 + \frac{h_r}{h_s} \right) u \left(t - \frac{y+2l}{a_N} \right) - \frac{a}{h_s^2} \left[-\frac{2(h_r h_s + h_r^2)}{h_s} \left(t - \frac{y+4l}{a_N} \right) + \right. \\
& + a \frac{h_r^2}{2} \left(t - \frac{y+4l}{a_N} \right)^2 + \frac{4h_r h_s + 3h_r^2 + h_s^2}{h_s^2} \left(1 - e^{-h_s \left(t - \frac{y+4l}{a_N} \right)} \right) - \left(\frac{h_r}{h_s} + 1 \right)^2 \cdot \\
& \cdot h_s \left(t - \frac{y+4l}{a_N} \right) e^{-h_s \left(t - \frac{y+4l}{a_N} \right)} \left. \right] u \left(t - \frac{y+4l}{a_N} \right) - \frac{a}{h_s^2} \left[\frac{3h_r^2 h_s + 3h_r^3}{h_s^2} \left(t - \frac{y+6l}{a_N} \right) - \frac{h_r^3}{h_s} \cdot \right. \\
& \cdot \frac{1}{2} \left(t - \frac{y+6l}{a_N} \right)^2 - 3 \frac{3h_r^2 + 2h_r^3 + h_r h_s^2}{h_s^3} \left(1 - e^{-h_s \left(t - \frac{y+6l}{a_N} \right)} \right) + 3h_r \left(\frac{h_r}{h_s} + 1 \right)^2 \cdot \\
& \cdot \left(t - \frac{y+6l}{a_N} \right) e^{-h_s \left(t - \frac{y+6l}{a_N} \right)} + \frac{1}{2} h_s^2 \left(\frac{h_r}{h_s} + 1 \right)^3 \left(t - \frac{y+6l}{a_N} \right)^2 e^{-h_s \left(t - \frac{y+6l}{a_N} \right)} \left. \right] u \left(t - \frac{y+6l}{a_N} \right)
\end{aligned}$$

When there is considered only the case of the tub starting from the shaft bottom the influence of the counterbalance rope may be neglected, and if ($h_1 = 0$) then $h_s = h + h_1 = h$ and $= h - h_1 = h$.

Now, when $h_s = h$ and $h_r = h$ are substituted in equations (6) and (7) the following formulae describing functions $g_0 \left(t + \frac{y}{a_N} \right)$ and $f_0 \left(t - \frac{y}{a_N} \right)$ were obtained:

$$g_0 \left(t + \frac{y}{a_N} \right) = \frac{a}{h^2} \left[\left[2h \left(t + \frac{y-2l}{a_N} \right) - \frac{1}{2} h^2 \left(t + \frac{y-2l}{a_N} \right)^2 + 2 \left(-1 + e^{-h \left(t + \frac{y-2l}{a_N} \right)} \right) \right] \right]. \quad (8)$$

$$\begin{aligned}
& \cdot u\left(t + \frac{y - 2l}{a_N}\right) + \left[-4h\left(t + \frac{y - 4l}{a_N}\right) + \frac{h^2}{2} \left(t + \frac{y - 4l}{a_N}\right)^2 + 8 \left(1 - e^{-h\left(t + \frac{y - 4l}{a_N}\right)}\right) \right] - \\
& -4h\left(t + \frac{y - 4l}{a_N}\right) e^{-h\left(t + \frac{y - 4l}{a_N}\right)} \Bigg] u\left(t + \frac{y - 4l}{a_N}\right) + \left[6h\left(t + \frac{y - 6l}{a_N}\right) - h^2 \frac{1}{2} \left(t + \frac{y - 6l}{a_N}\right)^2 - \right. \\
& \left. - 24 \left(1 - e^{-h\left(t + \frac{y - 6l}{a_N}\right)}\right) \right] + 12h\left(t + \frac{y - 6l}{a_N}\right) e^{-h\left(t + \frac{y - 6l}{a_N}\right)} + \\
& \left. + 4h^2 \left(t + \frac{y - 6l}{a_N}\right)^2 e^{-h\left(t + \frac{y - 6l}{a_N}\right)} \right] u\left(t + \frac{y - 6l}{a_N}\right) \Bigg\} \\
f_0\left(t - \frac{y}{a_N}\right) &= \frac{a}{h^2} \left\{ -\frac{a}{2} \left(t - \frac{y}{a_N}\right)^2 + \right. \\
& + \left[2h\left(t - \frac{y + 2l}{a_N}\right) \frac{1}{2} h^2 \left(t - \frac{y + 2l}{a_N}\right)^2 + 2 \left(-1 + e^{-h\left(t - \frac{y + 2l}{a_N}\right)}\right) \right] \Bigg\}. \tag{9} \\
& \cdot u\left(t - \frac{y + 2l}{a_N}\right) - \left[-4h\left(t - \frac{y + 4l}{a_N}\right) + \frac{h^2}{2} \left(t - \frac{y + 4l}{a_N}\right)^2 + 8 \left(1 - e^{-h\left(t - \frac{y + 4l}{a_N}\right)}\right) \right] - \\
& -4h\left(t - \frac{y + 4l}{a_N}\right) e^{-h\left(t - \frac{y + 4l}{a_N}\right)} \Bigg] u\left(t - \frac{y + 4l}{a_N}\right) - \left[6h\left(t - \frac{y + 6l}{a_N}\right) - h^2 \frac{1}{2} \left(t - \frac{y + 6l}{a_N}\right)^2 - \right. \\
& \left. - 24 \left(1 - e^{-h\left(t - \frac{y + 6l}{a_N}\right)}\right) \right] + 12h\left(t - \frac{y + 6l}{a_N}\right) e^{-h\left(t - \frac{y + 6l}{a_N}\right)} + \\
& \left. + 4h^2 \left(t - \frac{y + 6l}{a_N}\right)^2 e^{-h\left(t - \frac{y + 6l}{a_N}\right)} \right] u\left(t - \frac{y + 6l}{a_N}\right) \Bigg\}
\end{aligned}$$

The formula (3a) does describe the displacement of any cross-section of the counterbalance rope in the case of the tub elevated from the bottom loading level when the function g_0 and f_0 were determined. The stress in any cross-section of lifting ropes that result from the elevation of the tub is:

$$\sigma(t, y) = E_N \frac{\partial v}{\partial y} = \frac{E_N}{a_N} \left[g'_0 \left(t + \frac{y}{a_N} \right) - f'_0 \left(t - \frac{y}{a_N} \right) \right] \quad (10)$$

Then, after relation (8) and (9) were used and after ordering we have:

$$\begin{aligned} \sigma(t, y) = & E_N \frac{a}{h^2} \left\{ -\frac{h^2}{4a_N} \left(t - \frac{y}{a_N} \right) u \left(t - \frac{y+2l}{a_N} \right) - \right. \\ & \left[\frac{2h}{a_N} - \frac{h^2}{4a_N} \left(t - \frac{y+2l}{a_N} \right) - \frac{2h}{a_N} e^{-h \left(t - \frac{y+2l}{a_N} \right)} \right] u \left(t - \frac{y+4l}{a_N} \right) + \\ & + \left[\frac{4h}{a_N} + \frac{h^2}{4a_N} \left(t - \frac{y+4l}{a_N} \right) + \frac{4h}{a_N} e^{-h \left(t - \frac{y+4l}{a_N} \right)} + \frac{4h^2}{a_N} \left(t - \frac{y+4l}{a_N} \right) e^{-h \left(t - \frac{y+4l}{a_N} \right)} \right] \cdot \\ & \cdot u \left(t - \frac{y+6l}{a_N} \right) + \left[\frac{6h}{a_N} - \frac{h^2}{4a_N} \left(t - \frac{y+6l}{a_N} \right) - \frac{12h}{a_N} e^{-h \left(t - \frac{y+6l}{a_N} \right)} - \right. \\ & - \frac{10h^2}{a_N} \left(t - \frac{y+6l}{a_N} \right) e^{-h \left(t - \frac{y+6l}{a_N} \right)} - \frac{4h^3}{a_N} \left(t - \frac{y+6l}{a_N} \right)^2 e^{-h \left(t - \frac{y+6l}{a_N} \right)} \Big] \cdot \\ & \cdot u \left(t - \frac{y+6l}{a_N} \right) + \left[\frac{2h}{a_N} + \frac{h^2}{4a_N} \left(t + \frac{y-2l}{a_N} \right) - \frac{2h}{a_N} e^{-h \left(t + \frac{y-2l}{a_N} \right)} \right] u \left(t + \frac{y-2l}{a_N} \right) + \\ & + \left[-\frac{4h}{a_N} + \frac{h^2}{4a_N} \left(t + \frac{y-4l}{a_N} \right) + \frac{4h}{a_N} e^{-h \left(t + \frac{y-4l}{a_N} \right)} + \frac{4h^2}{a_N} \left(t + \frac{y-4l}{a_N} \right) e^{-h \left(t + \frac{y-4l}{a_N} \right)} \right] \cdot \\ & \cdot u \left(t + \frac{y-4l}{a_N} \right) + \left[\frac{6h}{a_N} + \frac{h^2}{4a_N} \left(t + \frac{y-6l}{a_N} \right) - \frac{12h}{a_N} e^{-h \left(t + \frac{y-6l}{a_N} \right)} - \frac{10h^2}{a_N} \left(t + \frac{6l}{a_N} \right) \right]. \end{aligned} \quad (11)$$

$$\cdot e^{-h\left(t+\frac{y-6l}{a_N}\right)} - \frac{4h^3}{a_N} \left(t + \frac{y-6l}{a_N} \right)^2 e^{-h\left(t+\frac{y-6l}{a_N}\right)} \Bigg] u\left(t + \frac{y-6l}{a_N}\right)$$

What's more, the dynamic surplus of the tub suspension load elevated with an acceleration a is:

$$\Delta S(t, y = l) = A_N \sigma(t, y = l) \quad (12)$$

Now, after operations described by the relation (12) we obtain:

$$\begin{aligned} & \Delta S(t, y) = A_N E_N \frac{a}{h^2} \\ & \left\{ -\frac{h^2}{4a_N} \left(t - \frac{l}{a_N} \right) u\left(t - \frac{l}{a_N}\right) - \left[\frac{2h}{a_N} - \frac{h^2}{4a_N} \left(t - \frac{3l}{a_N} \right) - \frac{2h}{a_N} e^{-h\left(t-\frac{3l}{a_N}\right)} \right] \right. \\ & \cdot u\left(t - \frac{3l}{a_N}\right) + \left[\frac{4h}{a_N} + \frac{h^2}{4a_N} \left(t - \frac{5l}{a_N} \right) + \frac{4h}{a_N} e^{-h\left(t-\frac{5l}{a_N}\right)} + \frac{4h^2}{a_N} \left(t - \frac{5l}{a_N} \right) e^{-h\left(t-\frac{5l}{a_N}\right)} \right]. \\ & \cdot u\left(t - \frac{5l}{a_N}\right) + \left[\frac{6h}{a_N} + \frac{h^2}{4a_N} \left(t - \frac{7l}{a_N} \right) - \frac{12h}{a_N} e^{-h\left(t-\frac{7l}{a_N}\right)} - \frac{10h^2}{a_N} \left(t - \frac{7l}{a_N} \right) - \right. \\ & \left. - \frac{4h^3}{a_N} \left(t - \frac{7l}{a_N} \right)^2 e^{-h\left(t-\frac{7l}{a_N}\right)} \right] u\left(t - \frac{7l}{a_N}\right) + \\ & + \left[\frac{2h}{a_N} - \frac{h^2}{4a_N} \left(t - \frac{l}{a_N} \right) - \frac{2h}{a_N} e^{-h\left(t-\frac{l}{a_N}\right)} \right] u\left(t - \frac{3l}{a_N}\right) + \\ & + \left[-\frac{4h}{a_N} + \frac{h^2}{4a_N} \left(t - \frac{3l}{a_N} \right) + \frac{4h}{a_N} e^{-h\left(t-\frac{3l}{a_N}\right)} + \frac{4h^2}{a_N} \left(t - \frac{3l}{a_N} \right) e^{-h\left(t-\frac{3l}{a_N}\right)} \right] u\left(t - \frac{3l}{a_N}\right) + \\ & + \left[\frac{6h}{a_N} + \frac{h^2}{4a_N} \left(t - \frac{5l}{a_N} \right) - \frac{12h}{a_N} e^{-h\left(t-\frac{5l}{a_N}\right)} - \frac{10h^2}{a_N} \left(t - \frac{5l}{a_N} \right) e^{-h\left(t-\frac{5l}{a_N}\right)} - \right. \end{aligned} \quad (13)$$

$$\left. -\frac{4h^3}{a_N} \left(t - \frac{5l}{a_N} \right)^2 e^{-h\left(t-\frac{5l}{a_N}\right)} \right] u\left(t - \frac{5l}{a_N}\right) \}$$

3. The effect of operational parameters on dynamical surplus in the suspension of the tub elevated from the shaft bottom

Dynamical surplus described by the relation (13) is the linear function of the set value of acceleration. Therefore the shape of the curve that shows the change of this surplus in time becomes invariable and possible corrections of values due to different starting accelerations could be made with regard to the simple relation:

$$\frac{a_i}{a_j} = \frac{S_i(t)}{S_j(t)} \quad (14)$$

where:

a_i, a_j — starting accelerations,

$S_i(t), S_j(t)$ — dynamical surplus of the tub suspensions loads corresponding with the above accelerations.

Fig. 4 shows the effect of starting acceleration on the value of dynamical surplus in the suspension of the tub elevated from the bottom loading level. It is presented in the form of starting time function made on the base of the relation (13).

The diagram (Fig. 4) has been constructed for the hoist facility having the parameters:

- total mass of the tub, $M_1 = 30\,000$ [kg],

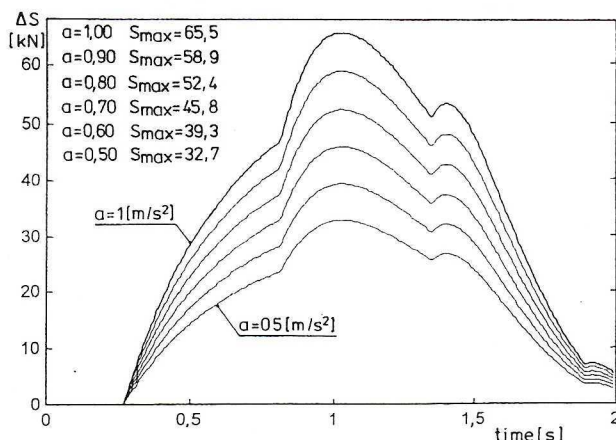


Fig. 4. The effect of starting acceleration on dynamical surplus in the tub suspension

Rys. 4. Wpływ przyspieszenia rozruchu na wartość nadwyżki dynamicznej w zawieszeniu naczynia

- total cross-section of supporting ropes, $A_N = 0.0028 \text{ [m}^2]$,
- longitudinal modulus of elasticity of ropes, $E_N = 1.1 \cdot 10^5 \text{ [MPa]}$,
- propagation velocity of the elastic deformation wave, $a_N = 3700 \text{ [m/s]}$,
- length of supporting ropes, $l_N = 1000 \text{ [m]}$.

The relation described by the formula (4) contains, in the parametrical form four quantities, which are essential for the considered assembly, i.e.:

- tension rigidity of supporting ropes; $A_N E_N$,
- propagation velocity of the elastic deformation in supporting ropes; a_N ,
- total discrete mass; M_1 .

The first and the second quantity ($A_N E_N$, a_N) are the material-design parameters of ropes.

The mass M_1 , owing to its variable component — M_u (usable mass) may be also considered as the parameter describing operational conditions of the hoist facility. Fig. 5 shows the family of suspension's load curves (dynamical surplus) as the time function for different discrete masses M_1 . The similar effects on this surplus exert other quantities of the formula (4).

The absolute, theoretically determined value of dynamical surplus in the tub suspension caused by starting of the facility has been increased with the increase of accelerated discrete mass (i.e. masses of the tub and mined material). Fig. 6 presents the example of such growth for the above-discussed parameters of the hoist facility.

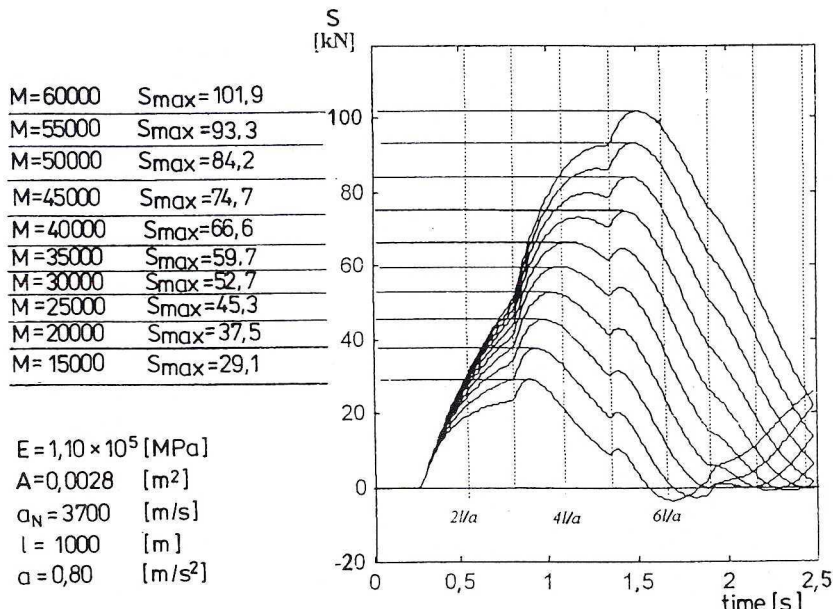


Fig. 5. The effect of the total mass on dynamical surplus in the suspension of the tub elevated from the shaft bottom

Rys. 5. Wpływ masy całkowitej na wartość nadwyżki dynamicznej w zawieszeniu naczynia podczas jego podnoszenia z podszybia

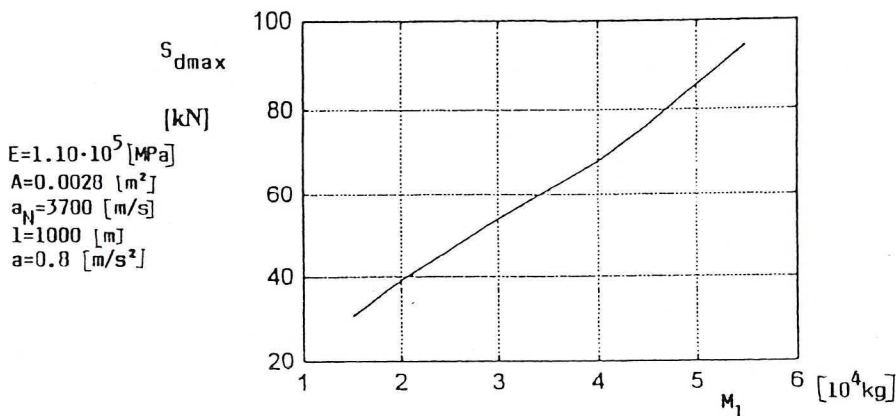


Fig. 6. The effect of discrete mass on the value of dynamical surplus in the suspension of the tub in its starting

Rys. 6. Wpływ masy dyskretnej na wartość nadwyżki dynamicznej w zawieszeniu naczynia podczas jego rozruchu

Anyway, as one can see in Fig. 7 the dynamical surplus related to the total static load considered in the classic manner, shows decrease and then rise. The significant difference between these two presentations consists in the visible change of that rise caused by the position of the local extreme on the time coordinate (see, Fig. 5). Dotted lines in Fig. 5 show the periods which determine the successive full transitions of the elastic deformation waves (calculated for the total length of the lifting rope ($y = l_N$), from the tub suspension to the point where the rope gets off the driving wheel ($y = 0$)). It is easy noticeable that positions of the local extreme of the function describing variation of dynamical surplus are moving with time and depend on the total mass. And what is more important from our point of view, their maximum values (for the assumed constant parameters of the assembly) fall in various time periods, which are determined by the time of the transition of the elastic deformation wave ($t = 2l_N/a_N$) trough the double length of the rope.

Then it could be stated as the recap that the relative dynamical surplus, considered in the above said way, has been decreasing when comes to the moment where the maximum value of the force relates to the subsequent local extreme (Fig. 5). For the range of operational parameters that is used in practice it is the time interval of three complete waves of the elastic deformation ($t = 6l_N/a_N$), which is essential for our considerations. It is illustrated by the results of the real object measurements presented in the next part.

The instantaneous length of the lifting rope engaged in the starting process, i.e. from the tub suspension to the point where the rope does leave the drive wheel still remains the steady parameter. Simulations of the increment of the suspension load dynamical surplus in relation to the position of the tub in the shaft have been performed on the base of the formula (13) and rather small length of the balance rope, assumed like before. The result of this simulation for the installation of the above said parameters is presented in

Fig. 8. The following lengths of the rope were used in the analysis of the starting process:
 $l_N = 1000 \text{ [m]}; 900 \text{ [m]}; 800 \text{ [m]}; 700 \text{ [m]}; 600 \text{ [m]}; 500 \text{ [m]}; 400 \text{ [m]}; 300 \text{ [m]}; 200 \text{ [m]}$.

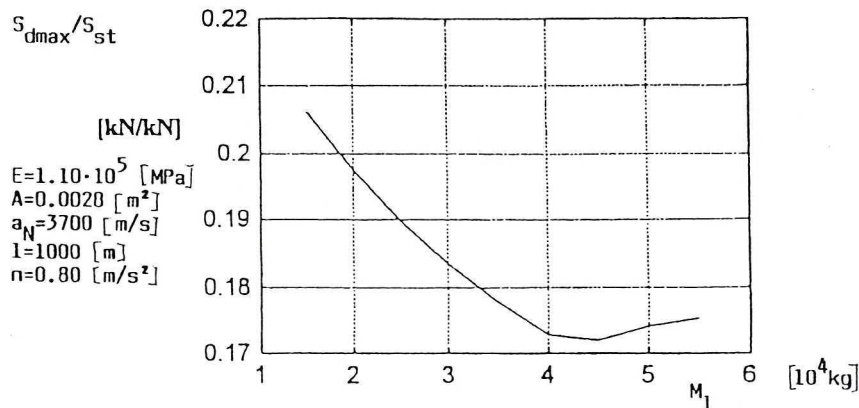


Fig. 7. The effect of discrete mass on the value of dynamical surplus in the tub suspension in the start phase

Rys. 7. Wpływ masy dyskretnej na wartość względnej nadwyżki dynamicznej w zawieszeniu naczynia podczas jego rozruchu

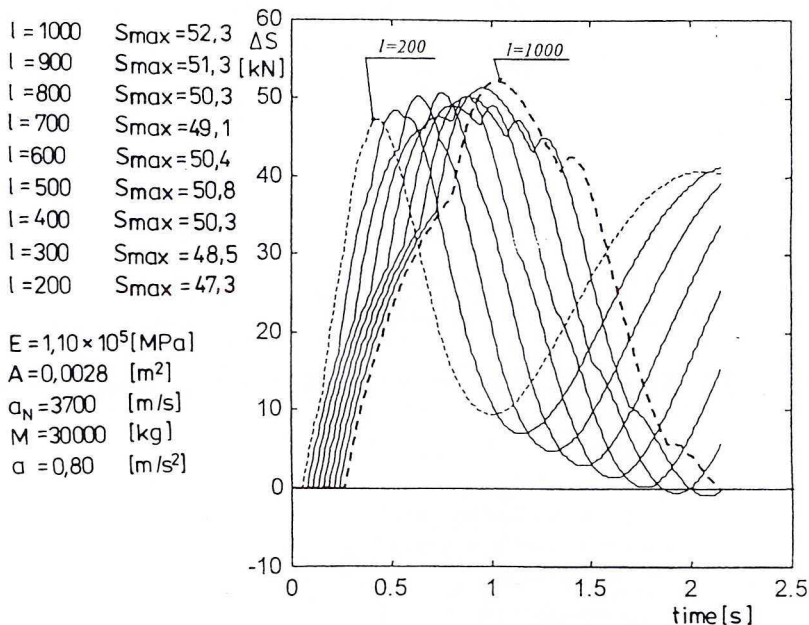


Fig. 8. The effect of lifting rope length on dynamical surplus of load in the tub suspension elevated with constant acceleration

Rys. 8. Wpływ długości liny nośnej na wartość nadwyżki dynamicznej obciążenia zawieszenia naczynia dla przypadku jego podnoszenia ze stałym przyspieszeniem

One can easily recognise the small effect of the lifting rope length on the maximum value of dynamical surplus of the tub suspension load in the starting process. The characteristic feature that follows decrease of the rope length is “smoothing” of the diagram of the tub suspension dynamical surplus. The change of the shape which is obviously visible in the diagram (Fig. 8) is the result of the propagation of the elastic deformation wave in predetermined ranges of time variable and position variable, what comes from the general structure of the solution (equation 3a).

When the distance of propagation of the wave effect is being decreased, the shorter is the time of secondary influence of the returned component of the wave on the incident wave characteristics, owing to the equation:

$$f_0\left(t - \frac{y}{a_N}\right) = -\frac{at^2}{2} - g_0\left(t + \frac{y}{a_N}\right) \quad (15)$$

As the consequence the calculation result of the assumed discrete — continuous model becomes similar to that of the discrete model (mass — spring).

4. Measurement of forces in tub suspensions during starting

The results of theoretical analysis have been verified in the experiment where forces in some elements of the mining hoist were measured during elevation of loaded tub from the bottom loading level. Tests were carried out in the real object i.e. one of the mining shafts of the Copper Mining-Metallurgical Corporation “Polish Copper” Inc. in Lubin, Poland. Fig. 9 shows the scheme of the “tower” hoist installation where the experiment was made.

4.1. General technological data of the “tower” hoist installation where the experiment was made

Type of the machine	4L-4000/2900
Drive D/C motor	2900 kW
Rated revolutions	77 rpm
Maximum velocity of the skip hoist	$V = 16$ [m/s]
Mass of the assembled empty tub with the suspension	$m_{ku} = 16\ 500$ [kg]
Useful mass	$m_{ku} = 17\ 000$ [kg]
Moments of inertia of rotating elements (GD^2)	
a) flywheel effect of the drum	$GD_s^2 = 1868.8$ [kNm ²]
b) flywheel effect the motor rotor	$GD_s^2 = 1275.3$ [kNm ²]
c) flywheel effect of the guide wheels	$GD_s^2 = 427$ [kNm ²]

The weight of guiding wheels ($D_K = 3.5$ m) reduced on the rope axis:

$$G_{KKz} = \frac{GD_K^2}{D_K^2} = \frac{474}{3.5^2} = 38.68 \text{ [kN]}$$

The weight of the drum ($D_B = 4.00$ m) reduced on the rope axis:

$$G_{Bz} = \frac{GD_B^2}{D_B^2} = \frac{1868.8}{4^2} = 116.8 \text{ [kN]}$$

The weight of the motor rotor ($D_R = 4.00$ m) reduced on the rope axis:

$$G_{Wz} = \frac{GD_s^2}{D_R^2} = \frac{12753}{4^2} = 79.7 \text{ [kN]}$$

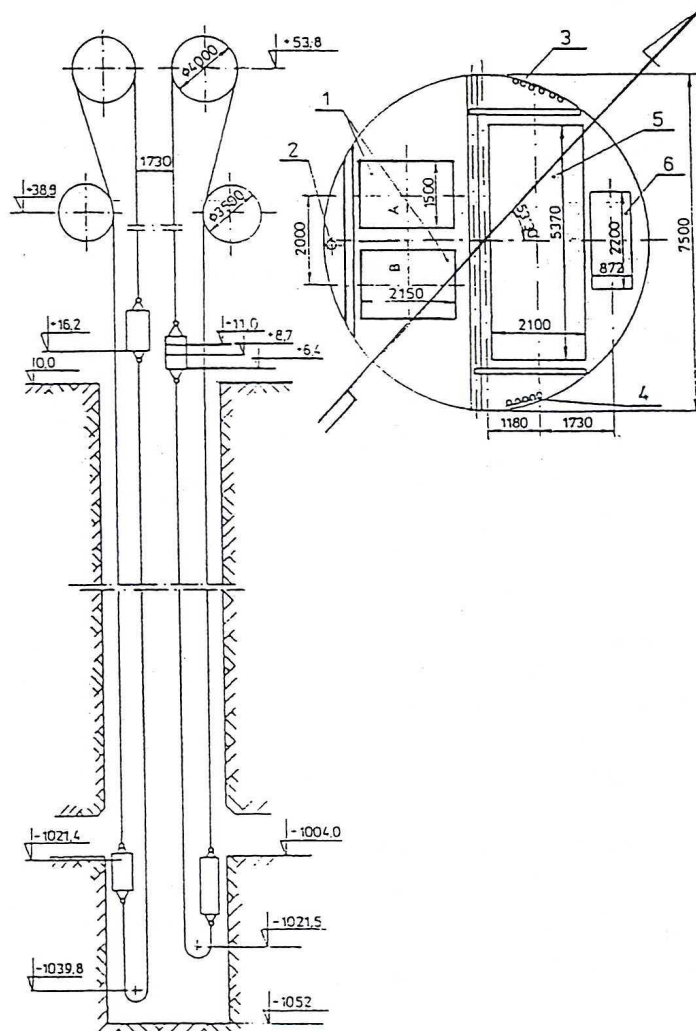


Fig. 9. The scheme of the hoist installation where the experiment was made
Rys. 9. Schemat urządzenia wyciągowego na którym przeprowadzono eksperyment

Reduced rotating masses in the tower:

$$M_0 = \frac{1}{g} \cdot (G_{KKz} + G_{Wz} + G_{Bz}) = \frac{1}{9.81} (38.68 + 116.8 + 79.7) = 23971 \text{ [kg]}$$

Lifting ropes:

- number of ropes $n_{LN} = 4$
- length of lifting ropes $l_N = 1230 \text{ [m]}$
- diameter of lifting ropes $\phi = 40 \text{ [mm]}$
- total section area of lifting ropes wires $A_N = 710 \text{ [mm}^2]$
- ultimate strength of lifting ropes $S_z = 4 \times 1154.0 = 4616 \text{ [kN]}$
- mass of 1 m of lifting ropes $q_N = 6.8 \text{ [kg/mb]}$

Counterbalance ropes:

- number of ropes $n_{lw} = 2$
- length of counterbalance ropes $l_w = 1200 \text{ [m]}$
- diameter of counterbalance ropes $\phi_w = 58 \text{ [mm]}$
- total section area of counterbalance ropes wires $A_w = 1545 \text{ [mm}^2]$
- ultimate strength of counterbalance ropes $S_{zw} = 155 \text{ [kN]}$
- mass of 1 m of balance ropes $q_w = 14 \text{ [kg/mb]}$

The load function of the suspension in the operational cycle has been determined with regard to the following parameters of the hoist facility:

- starting acceleration $a_1 = 0.8 \text{ [m/s]}$
- braking deceleration $a_2 = 1.0 \text{ [m/s}^2]$
- propagation velocity of the elastic deformation wave in lifting ropes $a_N = 3700 \text{ [m/s]}$

$$\sum A_N = 4A_N = 4 \cdot 710 = 2840 \text{ [mm}^2] = 2840 \cdot 10^{-6} \text{ [m}^2]$$

$$l_N = 1230 \text{ [m]}$$

$$E_N = 1.1 \cdot 10^5 \text{ [N/m}^2]$$

$$M_1 = m_u + m_{ku} = 16\ 500 + 17\ 000 = 33\ 500 \text{ [kg]}$$

$$l_{N1} = 42.8 \text{ [m]}$$

- weight of the part of the counterbalance rope for two positions of the skip:
 - extreme bottom position for the length of the part of balance rope in the shaft sump $l_{wr} = 18 \text{ [m]}$:

$$G_{Wr} = 2 \cdot l_{wr} \cdot q_w \cdot g = 2 \cdot 18 \cdot 14 \cdot 9.81 = 4.94 \text{ [kN]}$$

- extreme upper position for the length of the balance rope $l_{wr} = 1248 \text{ [m]}$:

$$G_{Wh} = 2l_{wn} \cdot q_w \cdot g = 2 \cdot 1248 \cdot 14 \cdot 9.81 = 342.80 \text{ [kN].}$$

4.2. The apparatus for measurement and recording of forces in tubs suspensions

Fig. 10 (Śmiejka 2000; Wolny 2000b) shows the scheme of the apparatus for measurement and recording forces in suspensions of tubs. Force strain gauges WSP of the following technological parameters were used in measurements:

- measuring range — 100 [kN],
- output voltage — 5 [V],
- accuracy class — 0.6,
- supply of the bridge — 5 [V].

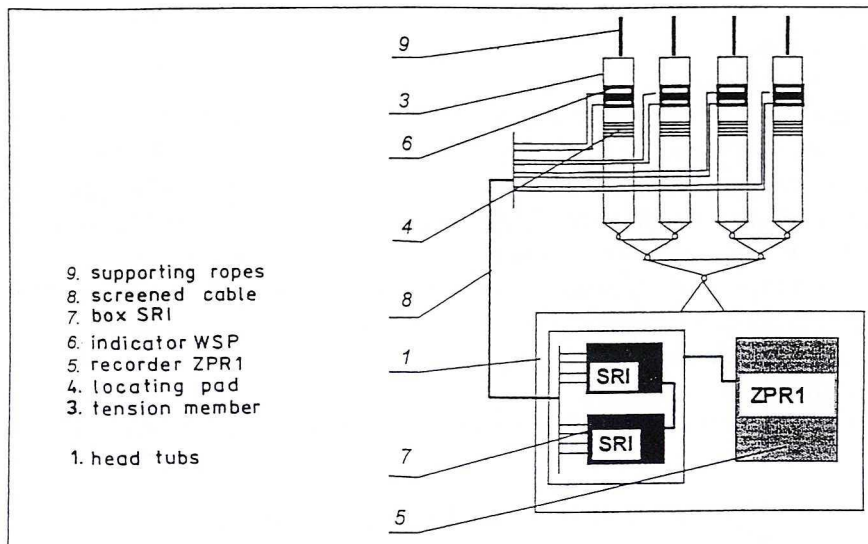


Fig. 10. Scheme of the measurement line and locations of force sensors

Rys. 10. Schemat toru pomiarowego i rozmieszczenia czujników siły

The assembly ZPR-1 supplied by the battery, type HP 2,6–12 V has been applied in recording signals from eight sensors (doubled in each string) having the sampling frequency 40 kHz. Recorded signals were converted into text files and then processed with the use of programme Matlab 5.2. Tangential velocity in the drive wheel has been recorded in all measurements.

4.3. Results of measurements of forces in tub suspensions during starting

There was recorded the load of the tub suspension in the regular operational cycle. Fig. 11 shows the diagram of the load of the tub suspension recorded in the typical operational cycle.

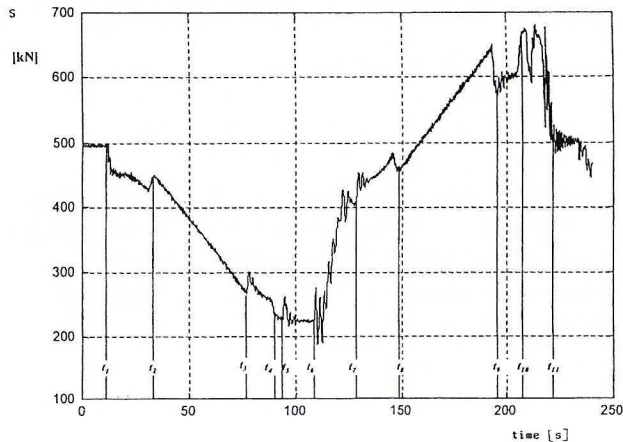


Fig. 11. Loads in the tub suspension during typical operational cycle

Rys. 11. Obciążenia zawieszenia naczynia w trakcie typowego cyklu eksploatacyjnego

Points marked on the time coordinate illustrate respectively:

- t_1 — start of the assembly with constant acceleration — a_1
 (going down of an empty tub),
 t_2 — begin of steady going down with constant velocity — V_0 ,
 t_3 — begin of braking with the constant deceleration — a_2 ,
 t_4, t_5, t_6 — arrival to the loading level and begin of loading,

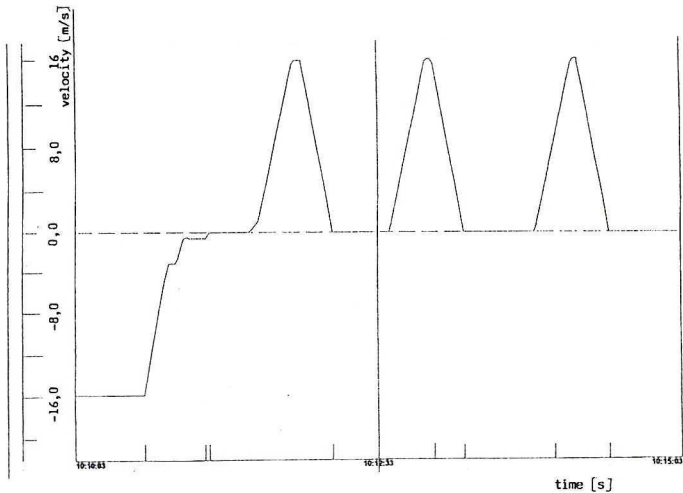


Fig. 12. Run diagram made during tests of loads in suspension of the tub started from three different levels with constant acceleration

Rys. 12. Wykres jazdy wykonany w trakcie badania obciążenia w zawieszeniu naczynia przy jego rozruchu ze stałym przyspieszeniem z trzech różnych poziomów

- t_7 — begin of the start with the constant acceleration — a_1
(going up of the loaded tub),
- t_8 — begin of steady going up with constant velocity — V_0 ,
- t_9 — begin of braking with constant deceleration — a_2 ,
- t_{10}, t_{11} — arrival to the unloading level and unloading.

Besides, loads in suspensions during starting period were tested in a more detailed way. Different values of loads in the suspension were tested for the tub lifted from three levels of the shaft, representing three lengths of lifting ropes.

The load in the tub suspension was recorded in the following sequence:

- start with constant acceleration,
- short part of steady state run,
- drive retardation with the set value of deceleration (without manoeuvre brake),
- standstill.

The above described sequence has been performed three times in the course of the single going up over the route of the shaft where were made experiments. It is illustrated in the run diagram presented in Fig. 12.

Fig. 13 shows some fragments of load diagram of the tub suspension in the starting stage.

The curves present the change of the tub suspension load of the total mass $M_1 = 30\,000 \text{ [kg]}$ elevated from different levels with the following lengths of lifting ropes:

- curve(a) — $l_N = 1000 \text{ [m]}$,
- curve(b) — $l_N = 680 \text{ [m]}$,
- curve(c) — $l_N = 360 \text{ [m]}$.

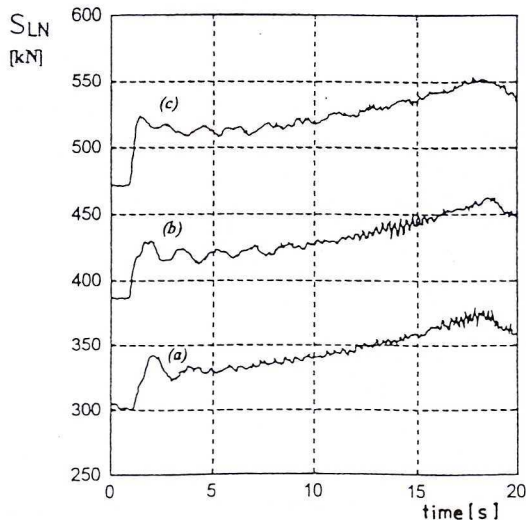


Fig. 13. Some fragments of the load of suspension during its starting

Rys. 13. Wybrane fragmenty obciążenia zawieszenia podczas jego rozruchu

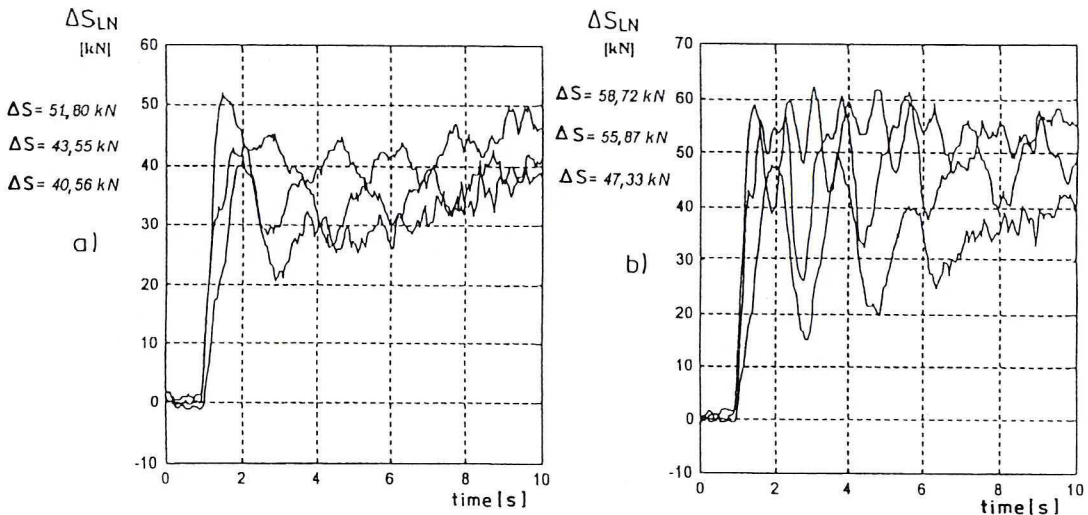


Fig. 14. Diagram of dynamical surplus of loads in tub suspensions, during starting of the assembly for two different total masses elevated from different depths
 a — $M_1 = 31\,000 \text{ [kg]}$; b — $M_1 = 41\,000 \text{ [kg]}$

Rys. 14. Wykres nadwyżek dynamicznych obciążenia w zawieszeniach naczynia podczas rozruchu układu dla dwóch różnych mas całkowitych podnoszonych z różnych głębokości
 a — $M_1 = 31\,000 \text{ [kg]}$; b — $M_1 = 41\,000 \text{ [kg]}$

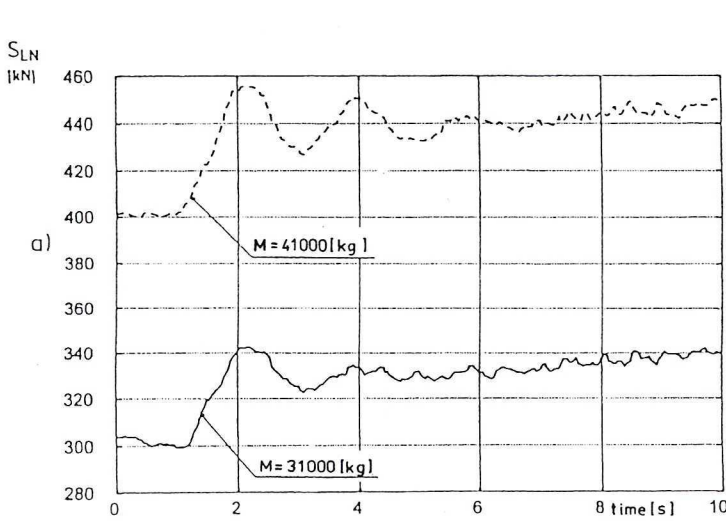


Fig. 15. Dynamical loads in tub suspensions during starting from the bottom loading level
 a — total load; b — absolute values of dynamic surpluses of loads

Rys. 15. Obciążenia dynamiczne w zawieszeniach naczyni podczas ich rozruchu z dolnego poziomu załadunkowego
 a — obciążenie całkowite; b — bezwzględne wartości nadwyżek dynamicznych obciążień

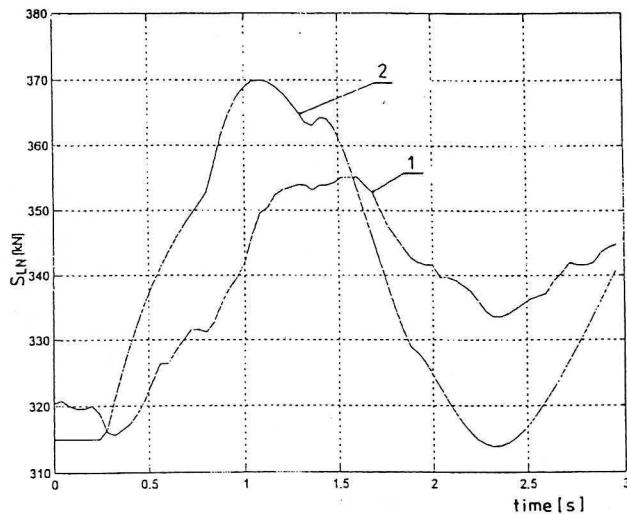


Fig. 16. Load of the tub ($M_1 = 31\,000$ [kg]) during its starting with constant acceleration from the shaft bottom obtained in experiment (curve 1) and in simulation based on the theoretical formula (relation 13, curve 2)

Rys. 16. Obciążenia naczynia ($M_1 = 31\,000$ [kg]) podczas jego rozruchu z podszybia ze stałym przyspieszeniem uzyskane na drodze eksperymentu (krzywa 1) oraz symulacji z wykorzystaniem wzoru teoretycznego (wzór (13), krzywa 2)

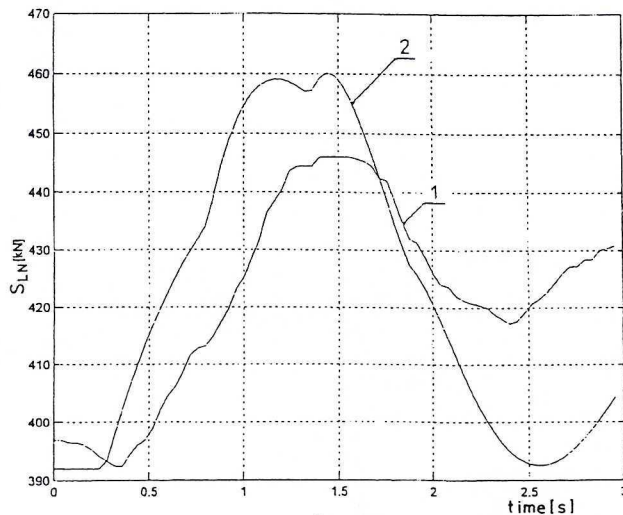


Fig. 17. Load of the tub ($M_1 = 41\,000$ [kg]) during its starting from the shaft bottom with constant acceleration obtained in experiment (curve 1) and in simulation based on theoretical formula (relation 13, curve 2)

Rys. 17. Obciążenia naczynia ($M_1 = 41\,000$ [kg]) podczas jego rozruchu z podszybia ze stałym przyspieszeniem uzyskane na drodze eksperymentu (krzywa 1) oraz symulacji z wykorzystaniem wzoru teoretycznego (wzór (13), krzywa 2)

Fig. 14 shows diagrams of dynamical surplus obtained in starting of the tub with the above said lengths of ropes but for two different total masses (part a — $M_1 = 31\ 000$ [kg], part b — $M_1 = 41\ 000$ [kg]).

Fig. 15a shows the absolute values of loads in tub suspensions during starting from the bottom loading level. The continuous line describes the facility of the total mass $M_1 = 31\ 000$ [kg] and dotted line that of total mass $M_1 = 41\ 000$ [kg]. Fig. 15b shows the diagram of dynamical surplus of the tub suspension loads whose absolute values are presented in Fig. 15a.

Figs. 16 and 17 show diagrams of the tub suspension loads during starting from the shaft bottom with constant acceleration, obtained in experiment (curve 1) and in simulation based on the theoretical formula (relation 13, curve 2), respectively with masses $M_1 = 31\ 000$ [kg] in Fig. 16 and $41\ 000$ [kg] in Fig. 17.

5. Concluding remarks

Relations, which were obtained describe the process of starting of the tub with constant acceleration. They are the result of theoretical analysis but were verified in the real object experiment, which confirmed that the simplifying assumptions were justified. Results of measurements of forces in the suspension of the tub in the starting period (Figs. 16 and 17) compared with results of theoretical analysis show adequate conformity from the technological point of view (maximum differences within 4–5%).

Anyway the dynamic surplus of loading in the suspension of the tub elevated with constant acceleration varies within more than ten percent (Figs. 14 and 15 show the extreme values within 10–20%).

It means that the loading of the tub suspension in the starting period, and especially in the condition of deep shafts, does not significantly affect the form of the tub loading in the regular operational cycle.

Finally it could be stated that the operational braking as well as starting of the tub from the shaft bottom, introduce “a disturbance” into the regular operation but from the point of view of the strength — fatigue calculations it does not cause any significant change.

REFERENCES

- Kaliski, 1987. Drgania i fale. PWN, Warszawa.
- Knop H., 1975. Wybrane zagadnienia z dynamiki urządzeń wyciągowych. ZN AGH. Elektryfikacja i Mechanizacja Górnictwa i Hutnictwa z. 67, Kraków.
- Śmiecja M., 2000. Analityczna i eksperymentalna ocena współczynników bezpieczeństwa wybranych elementów kopalnianego urządzenia wyciągowego. Praca doktorska, AGH, Kraków.
- Wolny S., Kjuregjan Ch., 1999. Analiza dynamiczna awaryjnych stanów pracy urządzenia wyciągowego z wykorzystaniem nieliniowego dyskretno-ciągłego modelu układu. Mechanika t. 18, z. 4, Kraków.

- Wolny S., 2000a. Obciążenia dynamiczne w zawieszeniach naczyń wydobywczych i lin wyrównawczych w warunkach hamowania bezpieczeństwa górnictwego urządzenia wyciągowego. Mechanika t. 19, z. 1, Kraków.
- Wolny S., 2000b. Wybrane problemy dynamiczne i wytrzymałościowe w eksploatacji górniczych urządzeń wyciągowych. Seria Monografic „Problemy Inżynierii Mechanicznej i Robotyki” Nr 1. Wyd. Wydział Inżynierii Mechanicznej i Robotyki AGH, Kraków.
- Wolny S., 2001. Theoretical and experimental analysis of loads in mining tubs suspensions in the condition of operational braking of mine hoist facility. Archives of Mining Sciences vol. 46, i. 1.

REVIEW BY: PROF. DR HAB. INŻ. TADEUSZ BANASZEWSKI, KRAKÓW

Received: 9 October 2000